Soft X-ray absorption spectroscopy of vanadium oxides[1]

M. Abbate[a]*, H. Pen[a], M.T. Czyżyk[a,2], F.M.F. de Groot[a], J.C. Fuggle[a,3], Y.J. Ma[b], C.T. Chen[b], F. Sette[b], A. Fujimori[c], Y. Ueda[d] and K. Kosuge[e]

[a]*Solid State Spectroscopy, University of Nijmegen, Toernooiveld 1, 6525 ED Nijmegen (The Netherlands)*
[b]*AT&T Bell Laboratories, Murray Hill, NJ 07974 (USA)*
[c]*Department of Physics, University of Tokyo, 7-3-1 Hongo, Bunkyo-ku, Tokyo 113 (Japan)*
[d]*Institute for Solid State Physics, University of Tokyo, Roppongi, Tokyo 106 (Japan)*
[e]*Department of Chemistry, University of Kyoto, Sakyo-ku, Kyoto 606 (Japan)*

(Received in final form 25 September 1992)

Abstract

We present the V2p and O1s X-ray absorption spectra of V_2O_3, VO_2 and V_2O_5. The V2p spectra show strong multiplet effects caused by large 2p–3d and 3d–3d Coulomb and exchange interactions. The spectra exhibit noticeable chemical shifts and completely different multiplets. The shapes of the multiplet are related to the symmetry and spin of the ground state. The V2p spectrum of V_2O_3 can be simulated by an atomic-multiplet calculation projected in the appropriate crystal field. The O1s spectra are related to unoccupied Op character mixed in the conduction band. The spectra reflect V3d bands near the edge and V4sp bands at higher energies. The V3d bands are split by crystal field effects. Changes in the relative intensities are related to differences in the metal–ligand hybridization. The extra dispersion of the V3d bands in V_2O_3 is attributed to larger metal–metal interactions. The O1s spectrum of VO_2 compares favorably to a symmetry-projected band structure calculation. Finally, the O1s spectra of VO_2 taken at room temperature (insulator phase) and at $T \approx 120\,°C$ (metallic phase) show clearly the splitting of the $V3d_\parallel$ band across the metal–insulator transition.

Introduction

The purpose of this paper is to investigate the electronic structure of V_2O_3, VO_2 and V_2O_5 by means of soft X-ray absorption spectroscopy (XAS). These materials have attracted much attention in the past because of their

---

[1] Dedicated to the memory of John C. Fuggle.
[2] Present address: Department of Applied Physics, University of Groningen, Nijenborgh 4, 9747 AG Groningen, Netherlands.
[3] Deceased.
* Corresponding author.

interesting electric and magnetic properties, as discussed below. Most of the experimental studies done until now were concerned with electron and X-ray spectroscopies which probe *occupied electronic states*. However, there is also a need for complementary studies of the *unoccupied electronic states* because these states include a major part of the dominant V3d bands. We show below that soft XAS can play a leading role in this area by providing information on the ground state, band dispersions, metal–ligand hybridizations and crystal field effects. In addition, XAS is able to reflect clearly changes in the $V3d_{\parallel}$ bands across the metal–insulator transition of VO_2.

The oxygen chemistry of vanadium is particularly rich and leads to compounds with very interesting physical and chemical properties [1]. The series V_2O_3, VO_2 and V_2O_5, for example, contains vanadium ions in different formal valencies and shows a broad range of electric and magnetic properties, including metal–insulator transitions [2–4]. V_2O_3 undergoes a first order transition at $T_c \approx 150\,K$ from an antiferromagnetic insulator phase at low temperature to a paramagnetic metallic state above T_c. In the metallic state, V_2O_3 presents the corundum structure (Al_2O_3) with strong metal–metal interactions along the hexagonal c axis and in the basal plane. VO_2 undergoes a first order transition at $T_c \approx 67\,°C$ from a non-magnetic insulator phase at low temperature to a paramagnetic metallic state above T_c. In the metallic state, VO_2 presents the rutile structure (TiO_2) with strong metal–metal interactions along the rutile c axis. Finally, V_2O_5 is a non-magnetic insulator and presents an orthorhombic structure. The ligand coordination around the V ions in V_2O_5 deviates from the ideal octahedra and direct metal–metal interactions are very weak.

The electronic structure of vanadium oxides were studied using various band structure [5–7] and cluster calculations [8,9]. The origin and nature of the metal–insulator transitions were often discussed in terms of model calculations [10–12]. Series of vanadium oxides were studied by means of X-ray photoelectron spectroscopy (XPS) [13–15]. The electron energy bands of V_2O_3 were analyzed using angle-resolved and resonant photoemission [16,17]. The electronic structure and the metal–insulator transition of a series of related vanadium oxides were recently studied by means of reflectance and photoemission spectroscopy [18].

In soft X-ray absorption, a shallow core electron absorbs a photon and is excited to unoccupied states above the Fermi level [19]. The X-ray absorption process for a simple metal is illustrated schematically in Fig. 1(a). There are two extreme regimes in soft XAS, which depend on the relative magnitude of intra-atomic interactions versus the dispersion of the respective band. In the first regime, the multipole interactions are small compared to the band width and the independent particle approach is a good starting point for the interpretation of the spectra. In these cases, the spectra resemble quite closely the local density of unoccupied states projected in
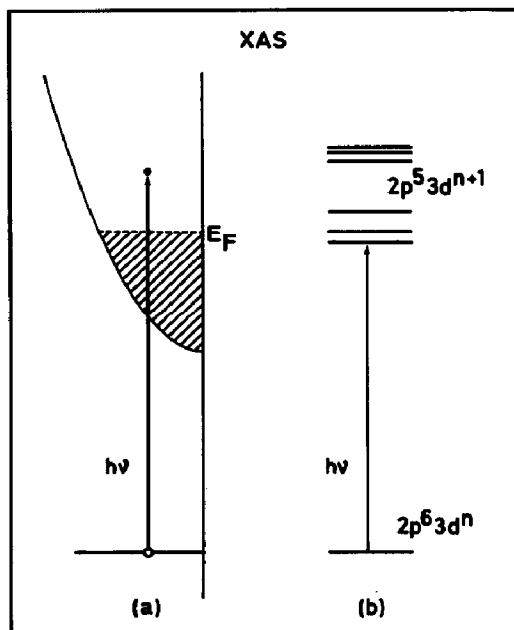
Fig. 1. (a) Schematic representation of the soft X-ray absorption process for a simple metal. (b) Soft X-ray absorption transition between states in transition metal 2p edges.

the appropriate symmetry. This approach yields good results in the O1s XAS spectra of some transition metal compounds. In the second regime, the interactions between the core hole and the valence electrons dominate and the spectra must be interpreted in terms of transitions from a well defined ground state to a set of excited states, as illustrated in Fig. 1(b). In these cases, the spectra usually present strong multiplet effects, which can be explained by atomic-like calculations. This approach accounts for the spectral shapes in the metal 2p XAS spectra of most transition metal compounds.

Experimental details

The measurements were carried out at the National Synchrotron Light Source (NSLS) in Brookhaven using the Dragon monochromator [20,21]. The energy resolution of the monochromator at the V2p and O1s edges (around 520 eV) was approximately 150 meV. The base pressure in the main chamber was in the low 10^{-10} Torr range. The spectra were collected using the total electron yield (TEY) mode and normalized to the maximum intensity. The samples were single crystals grown by the chemical vapour transport (CVT) method. Two different VO_2 spectra are presented here: one was taken at room temperature (insulator phase) and the other at $T \approx 120\,^\circ C$ (metallic phase).
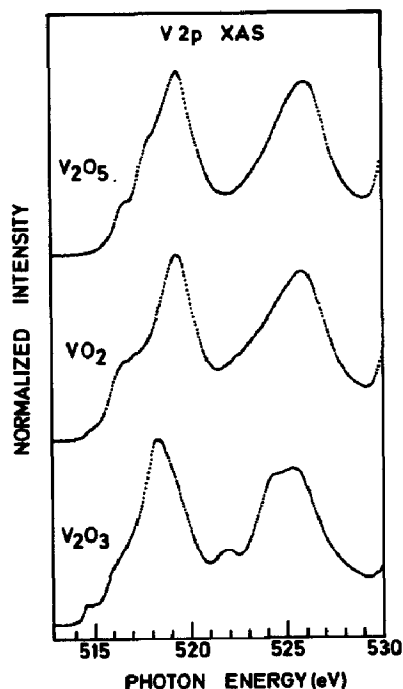
Fig. 2. V2p X-ray absorption spectra of V_2O_3, VO_2 and V_2O_5.

Results and discussion

The V2p and O1s X-ray absorption spectra corresponding to V_2O_5 and the metallic phases of VO_2 ($T \approx 120\,°C$) and V_2O_3 (room temperature) are presented and discussed first. The changes in the O1s spectra of VO_2 across the metal–insulator transition (room temperature versus $T \approx 120\,°C$) are analyzed later.

Vanadium 2p XAS spectra of V_2O_3, VO_2 and V_2O_5

The V2p X-ray absorption spectra of V_2O_3, VO_2 and V_2O_5 are shown in Fig. 2. The spectra correspond to on-site transitions from a well defined ground state ($2p^6 3d^n$) to one of the possible final states ($2p^5 3d^{n+1}$) allowed by the dipole selection rule. The spectra show two broad structures, around 518 and 525 eV approximately, which can be attributed, in a first approximation, to the $2p_{3/2}$ and $2p_{1/2}$ levels respectively. However, the interactions between the core hole and the valence electrons in the final state are of the order of the spin–orbit splitting of the 2p level. The breakdown of the jj coupling scheme causes a noticeable redistribution of the spectral weight throughout the entire spectra; the transfer of spectral weight from the $2p_{3/2}$ to the $2p_{1/2}$ region is particularly clear (see Fig. 2). In addition, the 2p–3d
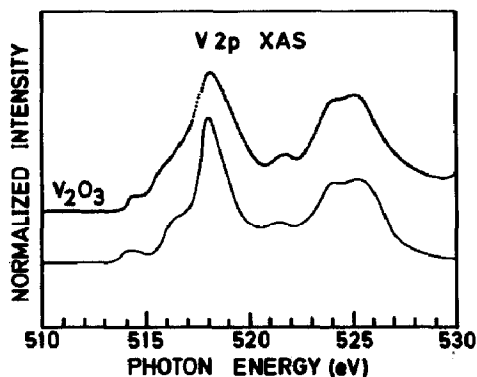
Fig. 3. Comparison between the V2p X-ray absorption spectrum of V_2O_3 and an atomic-multiplet simulation calculated assuming a $t_{2g}^2(^3T_1)$ ground state ($10\,Dq = 1.5\,eV$).

and 3d–3d Coulomb and exchange interactions are large in comparison to the dispersion of the 3d bands and this causes strong multiplet effects.

The V2p spectra present noticeable chemical shifts and completely different multiplets (see Fig. 2). These changes provide interesting information on the electronic structure of these materials. The chemical shifts are caused by changes in the average electrostatic energy at the vanadium sites due to differences in the 3d count and are characteristic of the different vanadium valencies in the series [22]. The shape of the spectra are dictated by the set of final states which can be reached from the ground state via the dipole selection rule. This means that the multiplets observed in the V2p spectra depend implicitly on the symmetry and spin of the ground state [23,24]. This dependence can be used, for instance, to study the changes in the electronic properties of transition metal compounds induced by substitution [25,26].

The experimental V2p XAS spectrum of V_2O_3 is compared in Fig. 3 to an atomic-multiplet calculation projected in octahedral symmetry. The theoretical spectrum was calculated assuming a $t_{2g}^2(^3T_1)$ ground state, the Slater integrals scaled down to 80% of their Hartree–Fock values and the crystal field strength parameter $10Dq$ set to 1.5 eV. The simulation was shifted by hand to obtain the best overall match with the experiment. The agreement in Fig. 3 is very good and illustrates the potential of soft XAS to determine the symmetry and spin of the ground state. A more accurate analysis should take into account the influence of configuration interactions and the contribution of crystal field components of lower symmetry.

Oxygen 1s XAS spectra of V_2O_3, VO_2 and V_2O_5

The O1s X-ray absorption spectra of V_2O_3, VO_2 and V_2O_5 are shown in Fig. 4. The spectra correspond to transitions from the O1s core level to
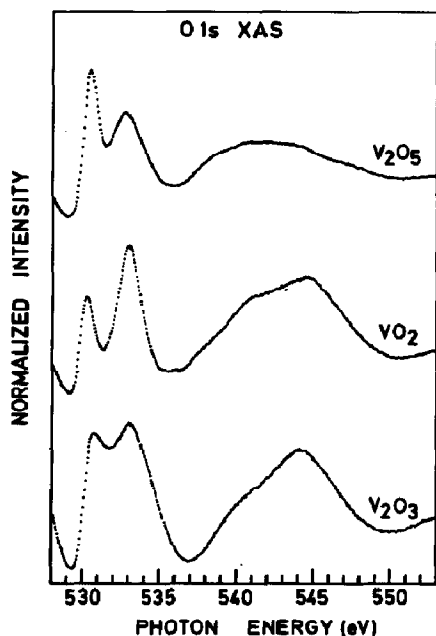
Fig. 4. O1s X-ray absorption spectra of V_2O_3, VO_2 and V_2O_5.

unoccupied Op character mixed in the conduction band. The absorption intensity, which should be very weak in a purely ionic picture, provides a good indication of covalency effects. The different features in the spectra correspond to bands of primary metal character. The main character of each band can be inferred from the parent molecular orbital levels [27–29]. The prominent doublets near the edge (around 530–537 eV) are attributed to V3d bands split by crystal field effects. The broad structures at higher energies (around 537–550 eV) are attributed to V4sp bands. The V4sp bands are pushed up in energy with respect to the V3d bands because of the relatively larger V4sp–O2p antibonding interactions.

The doublet splitting in the O1s spectra provide an indirect indication of crystal field effects on the V3d bands. These splitting contain an ionic as well as a covalent contribution and can be explained qualitatively in terms of symmetry considerations. The upper band corresponds to V3d orbitals which point towards the ligands. These states appear at higher energies because they have a larger overlap with the negative charge concentrated at the ligand sites and because they form relatively stronger σ antibonding combinations with O2p orbitals. The lower band corresponds to orbitals which point in between ligands. These have a smaller overlap with ligand sites and form weaker π antibonding combinations.

The intensity of the different structures in the O1s spectra are related to the strength of the metal–ligand hybridization in each molecular orbital
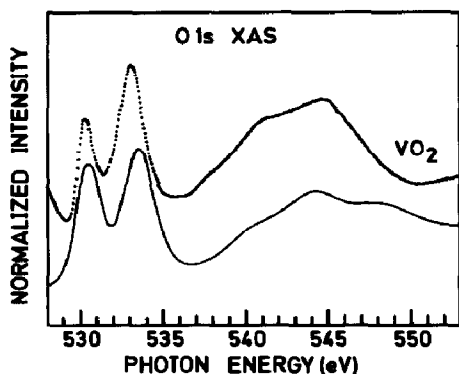
Fig. 5. Comparison between the O1s X-ray absorption spectrum of VO_2 and a density of unoccupied states projected on Op symmetry calculated by the LSW method.

derived band. For example, Fig. 4 shows that the relative intensity of the V3d bands increase with respect to the V4sp bands as one goes from V_2O_3 to V_2O_5. This relative enhancement is related to a larger V3d–O2p hybridization for higher V valencies. This trend indicates also that the contribution of the V3d electrons to the bonding increases from V_2O_3 to V_2O_5.

Figure 4 shows that the V3d bands of V_2O_3, as reflected by the O1s spectra, appear broader than those of VO_2 and V_2O_5. The broadening in the spectra are mainly given by the dispersion of the V3d bands [30]. Part of the V3d dispersion in these oxides is given by indirect interactions via the ligands (V3d–O2p–V3d). This mechanism explains why the e_g band, which is related to stronger V3d–O2p σ bonds, is usually broader than the t_{2g} band. The extra broadening in the case of V_2O_3 is attributed to larger direct interactions (V3d–V3d) because of the shorter V–V distances in this compound.

Figure 5 compares the O1s spectrum of VO_2 in the metallic phase and a broadened Op-projected density of states (DOS). The DOS was calculated using the localized spherical wave (LSW) method with an extended basis set [31]. The theoretical result was shifted by hand to obtain the best overall match with the experimental spectrum. The agreement is very good except for the Ti4s band region around 547–550 eV [32]. This shows that band structure calculations can give reasonable results for some of the early transition metal oxides. This is somehow unexpected and even puzzling, because the 3d–3d interactions in these compounds cannot be neglected.

Changes in the O1s XAS spectra of VO_2 across the metal–insulator transition

Figure 6 shows the O1s soft X-ray absorption spectra of VO_2 taken at room temperature (insulator phase) and at T $\approx$ 120 °C (metallic phase) [33].
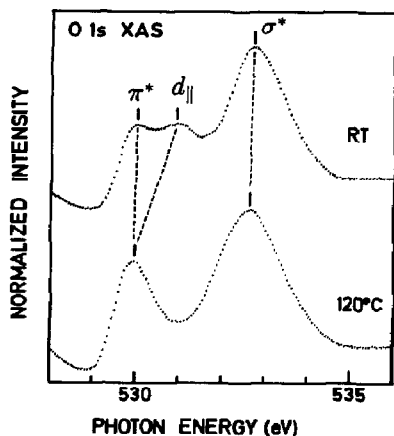
Fig. 6. O1s X-ray absorption spectra of VO_2 taken at room temperature (insulator phase) and at $T \approx 120\,°C$ (metallic phase). The different peaks in the spectra are labelled according to the approximate molecular orbital classification scheme.

Only the regions related to V3d bands are shown here because the V4sp bands show hardly any change. The origin of the different peaks in the spectra can be explained in terms of molecular orbital (MO) and crystal field ideas, as proposed by Goodenough [34].

The top panel of Fig. 7 shows how VO_6 octahedra share edges in the undistorted rutile structure (metallic phase). In this coordinate system,
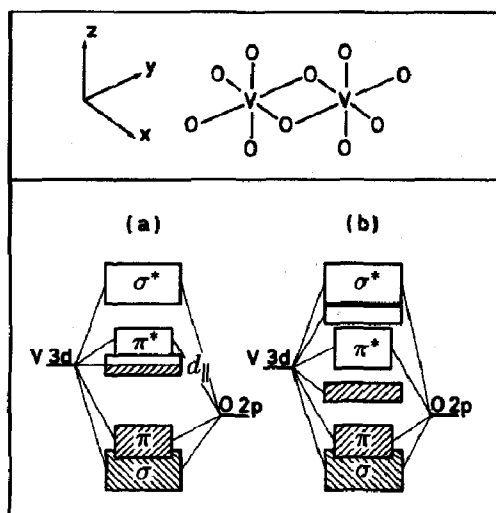

Fig. 7. Top panel, schematic representation of the VO_6 octahedra in the undistorted rutile structure. Lower panel, approximate electronic structure of VO_2 in terms of MO derived bands: (a) undistorted structure (metallic) and (b) distorted structure (insulator).

V3d orbitals of $3z^2 - r^2$ and $x^2 - y^2$ symmetry point towards the ligands and form σ bands with O2p orbitals. In contrast, orbitals of xz and yz symmetry point in between the ligands and form π bands. Finally, xy orbitals point towards the next nearest neighbor V site and form the $d_\parallel$ band. The schematic electronic structure of metallic VO_2 based on this MO analysis is shown in Fig. 7(a). The metallic behavior is the consequence of the partially filled $d_\parallel$ band overlapping the π^* bands. In the insulator phase below T_c, a complex distortion changes the crystallographic structure and forms pairs of V atoms. At the same time, the $d_\parallel$ band is split in two components because of band structure and electron repulsion effects, as illustrated in Fig. 7(b). The filling of the lower band, which correspond to singlet formation within the V–V pairs, explains both the drop of the metallic conductivity and the absence of magnetic moments below T_c.

The various peaks in the O1s spectra are labelled according to this approximate MO classification scheme (see Fig. 6). The band structure effects and the electron repulsion interactions within the V–V pairs are strong enough to push up the unoccupied part of the $d_\parallel$ band approximately 1 eV above the π^* bands edge. In contrast, the weak shift of the σ^* bands, approximately 0.2 eV, reflects smaller electron–lattice interactions and the relatively non-bonding π^* bands hardly shift at all. Optical data and photoemission spectra indicate that the band gap in the insulator phase is approximately 0.7 eV [18]; in combination with the present results this gives a splitting of approximately 2 eV between the lower and upper $d_\parallel$ band. In conclusion, the main changes in the electronic structure of VO_2 across the metal–insulator transition occur in the $d_\parallel$ band.

The changes in the electronic structure are caused by *both* electron–electron repulsion and electron–lattice interactions. On the one hand, band structure effects can explain the band gap opening in terms of the reduced symmetry and the ensuing changes in the hybridization [6]. On the other hand, cluster calculations suggest that electron correlation effects contribute approximately 0.7–0.9 eV to the splitting of the $d_\parallel$ band [8]. Indeed, it is difficult to explain the large splitting of the $d_\parallel$ band in terms of band structure effects alone. Finally, the metal–insulator transition in VO_2 is basically driven by the decrease in the electronic energy caused by the filling of the lower $d_\parallel$ band.

Summary and conclusions

In summary, we have presented here the V2p and O1s X-ray absorption spectra of V_2O_3, VO_2 and V_2O_5. The shape of the multiplets in the V2p spectra are related to the symmetry and spin of the ground state. The V2p spectrum of V_2O_3 can be simulated by an atomic-multiplet calculation projected in the appropriate crystal field. The O1s spectra are related to

unoccupied Op character mixed in the conduction band. The spectra reflect V3d bands near the edge and V4sp bands at higher energies. The O1s spectra provide information on crystal field effects, metal–ligand hybridization and the dispersion of the V3d bands. The O1s spectrum of VO_2 is compared to a symmetry-projected band structure calculation. The O1s spectra of VO_2 taken at room temperature (insulator phase) and at $T \approx 120\,°C$ (metallic phase) show clearly the splitting of the V3d$_\parallel$ band across the metal–insulator transition.

Acknowledgments

References

1   A.F. Wells, Structural Inorganic Chemistry, Clarendon, Oxford, 1975.
2   D. Adler, Rev. Mod. Phys., 40 (1968) 714.
3   J.B. Goodenough, Progress in Solid State Chemistry, Vol. 5, Pergamon, Oxford, 1971, p. 145.
4   N.F. Mott, Metal–Insulator Transition, Taylor and Francis, London, 1974.
5   E. Caruthers, L. Kleinman and H.I. Zhang, Phys. Rev. B, 7 (1973) 3753.
6   E. Caruthers and L. Kleinman, Phys. Rev. B, 7 (1973) 3760.
7   M. Gupta, A.J. Freeman and D.E. Ellis, Phys. Rev. B, 16 (1977) 3338.
8   C. Sommers, R. de Groot, D. Kaplan and A. Zylbersztejn, J. Phys. (Paris), 36 (1975) L157.
9   M. Gupta and D.E. Ellis, Phys. Rev. B, 13 (1976) 3405.
10 A. Zylbersztejn and N.F. Mott, Phys. Rev. B, 11 (1975) 4383.
11 A. Holz, K.A. Penson and K.H. Bennemann, Phys. Rev. B, 16 (1977) 3999.
12 D. Paquet and P. Leroux-Hugon, Phys. Rev. B, 22 (1980) 5284.
13 C. Blaaw, F. Leenhouts, F. van der Woude and G.A. Sawatzky, J. Phys. C, 8 (1975) 459.
14 G.A. Sawatzky and D. Post, Phys. Rev. B, 20 (1979) 1546.
15 C.N.R. Rao, D.D. Sarma, S. Vasudevam and M.S. Hedge, Proc. R. Soc. London, Ser. A, 367 (1979) 239.
16 K. Smith and V.E. Henrich, Phys. Rev. B, 38 (1988) 5965.
17 K. Smith and V.E. Henrich, Phys. Rev. B, 38 (1988) 9571.
18 S. Shin, S. Suga, M. Taniguchi, M. Fujisawa, H. Kanzaki, A. Funimori, H. Daimon, Y. Ueda, K. Kosuge and S. Kachi, Phys. Rev. B, 41 (1990) 4993.
19 J.C. Fuggle and J.E. Inglesfield, Unoccupied Electronic States, Springer-Verlag, Berlin, 1992.
20 C.T. Chen, Nucl. Instrum. Methods A, 256 (1987) 595.
21 C.T. Chen and F. Sette, Rev. Sci. Instrum., 60 (1989) 1616.
22 J. Taftø and O.L. Krivanek, Phys. Rev. Lett., 48 (1982) 560.
23 F.M.F. de Groot, J.C. Fuggle, B.T. Thole and G.A. Sawatzky, Phys. Rev. B, 41 (1990) 928.

24   F.M.F. de Groot, J.C. Fuggle, B.T. Thole and G.A. Sawatzky, Phys. Rev. B, 42 (1990) 5459.

25   M. Abbate, F.M.F. de Groot, J.C. Fuggle, A. Fujimori, Y. Tokura, Y. Fujishima, O. Strebel, M. Domke, G. Kaindl, J. van Elp, B.T. Thole, G.A. Sawatzky, M. Sacchi and N. Tsuda, Phys. Rev. B, 44 (1991) 5419.

26   M. Abbate, F.M.F. de Groot, J.C. Fuggle, A. Fujimori, O. Strebel, F. Lopez, M. Domke, G. Kaindl, G.A. Sawatzky, M. Takano, Y. Takeda, H. Eisaki and S. Uchida, Phys. Rev. B, 46 (1992) 4511.

27   D.W. Fischer, J. Appl. Phys., 41 (1970) 3561.

28   D.W. Fischer, J. Phys. Chem. Solids, 32 (1971) 2455.

29   D.W. Fischer, Phys. Rev. B, 5 (1972) 4219.

30   The contributions to the broadening coming from the O1s core hole lifetime, phonon effects and the experimental resolution are much smaller and can be neglected in a first approximation.

31   M. Grioni, M.T. Czyzyk, F.M.F. de Groot, J.C. Fuggle and B.E. Watts, Phys. Rev. B, 39 (1989) 4886.

32   This Ti4s band is expected to become broader and less intense in a calculation where more higher energy states are included in the hamiltonian.

33   M. Abbate, F.M.F. de Groot, J.C. Fuggle, Y.J. Ma, C.T. Chen, F. Sette, A. Fujimori, Y. Ueda and K. Kosuge, Phys. Rev. B, 43 (1991) 7263.

34   J.B. Goodenough, J. Solid State Chem., 3 (1971) 490.